OPTIMISATION OF A SOLAR-POWERED HIGH ALTITUDE LONG ENDURANCE UAV WITH COMPOSITE WINGS

Olivier Montagnier, Laurent Bovet*
Flight Dynamics Team
Research centre of the French Air Force
Base Aérienne 701, 13661 Salon air, France
olivier.montagnier@inet.air.defense.gouv.fr

Abstract

High altitude high endurance solar powered UAV can be a solution for many missions. The design complexity is due to the very high altitudes expected and the low available capacity to supply the engines. Optimisation carried out here consists in maximising the payload for a fixed total mass. It requires mass model for each constitutive part of the aircraft. In particular, the mass of the wing is minimised by the use of composite materials and by tolerate a large flexibility. An new analytical mass model is proposed here very useful for this particular application. Optimisation shows the existence of the UAV in a cruise speed versus lift coefficient diagram. This one revealed an optimal solution having a payload of about 13 % of the total mass of 220 kg for a 24 m wing span.

1 Introduction

Solar-powered HALE (High Altitude High Endurance) UAV could be a complement for many scientific missions like earth monitoring (early forest fire mapping, flood control, hurricane tracking and agriculture remote sensing [1]), an alternative for surveillance mission (security and border controls) and a substitute for telecommunication satellites (operates in stationary orbits or at great range, low cost platform, low cost maintenance, ...). For this kind of operation, these UAVs should have the capabilities to flight over the civil transport traffic at least weeks to months. Since the 90s, several works were carried out on the design of these UAVs [2, 3, 4, 5]. The NASA ERAST program (Environmental Research Aircraft and Sensor Technology) was the main project on these problematics. The NASA showed the possibilities of solar-powered HALE UAVs with several platforms like "Pathfinder Plus" prototype which has reached an altitude of 24 km [6] but this success was decreased by the crash of the "Helios" prototype [7]. The "NASA Mishap Investigation" concluded to an undamped pitch oscillation at 3 000 ft altitude due to the "complex interactions between the aerodynamic, structural, stability and control and propulsion systems on a flexible aircraft". Therefore, main design variables like wing aspect ratio, cruise speed, wing loading, geometry, energy storage system for the night flight ... are not enough established.

Design difficulty are due to the very high altitude expected (more than 20 km) and the low available energy to supply motors, energy storage system and electric payload. A simply power analysis for a fixed total mass shows that cruise speed of these future UAVs must be low. Air density at 20 km comparatively to 0 km is 10 more lower. Therefore, wing surface must be very large. Feasibility can be obtain by decreasing dramatically structural mass of the aircraft. Firstly, wing mass can be reduced using composite materials and tolerating high flexibility. Secondly, aircraft mass can be reduced by suppressing lifting and control surfaces like tail, for example, by using electric motors to control yaw and stable aerofoil. Fig. 1 shows an artist view of the solar-powered HALE UAV considered here.

*New address: Airbus France, 316 route de Bayonne, 31060 Toulouse cedex 03, France.

Copyright © 2009 by M. O. Montagnier. Published by the EUCASS association with permission.

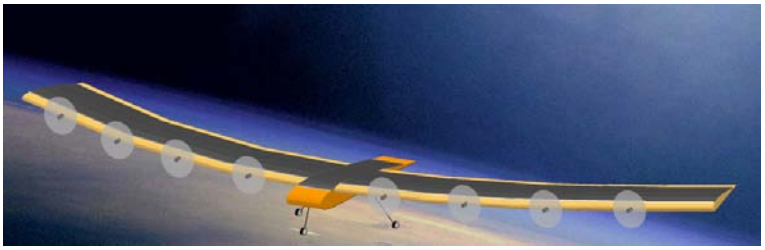

Figure 1: Artist view of the solar-powered HALE UAV

Margins are very small. Optimised UAV should be obtain with multidisciplinary optimisation tools (MDO). The aim of this work is to compute optimal parameters of a UAV with straight wings for a fixed wing aspect ratio and a fixed mass. Unlike classical design approach, size and cruise speed are the optimised parameters to maximise payload. Mass models, which are critical points of this kind of optimisation, are considered accurately. In particular, a composite wing mass model is proposed. Wing technology consists of a tubular beam with hybrid carbon/epoxy plies and constant cross section. This analytical model is well adapted to a wide range of solar-powered HALE UAV with straight wings.

2 Atmospheric and solar radiance models

Design of a Solar-powered HALE need to take account of wind, solar radiation and atmosphere.

Main mission of this aircraft will consist in stationary flight. Therefore, cruise speed must be higher than air speed in the flight area. A study of Romeo *et al.* [4] shows wind speed in Italy is twice as much lower at 20 km than at 10 km, maximum gust and average wind are equal to 40 $m.s^{-1}$ and 26 $m.s^{-1}$, respectively. These values are taken as a reference.

The solar radiance model gives the power receive by the photovoltaic cells per unit area, $\overline{P_S}$. This radiance power is a function of aircraft altitude h, of aircraft latitude $\hat{\lambda}$, of day of the year $\hat{j}$ and solar time $\hat{h}$, which can be written in the following form [2] :

$$\overline{P_S} = C_S \Delta_S \alpha_S \cos i_S \sin\left(\pi \frac{\hat{h} - \hat{h}_{sunrise}(\hat{j})}{\hat{h}_{sunset}(\hat{j}) - \hat{h}_{sunrise}(\hat{j})}\right)$$

with

$$\Delta_S = 1 + 0.033 \cos \frac{2\pi \hat{j}}{365}\,; \quad i_S = \hat{\lambda} - 23.45 \sin\left(\frac{2\pi\,(284 + \hat{j})}{365}\right)$$

$$\alpha_S = \frac{1}{2}\left(e^{-0.65 m(h,i_S)} + e^{-0.095 m(h,i_S)}\right)\,; \quad m(h, i_S) = \frac{p(h)}{p_o}\left(\sqrt{1229 + (614 \cos i_S)^2} - 614 \cos i_S\right)$$

where C_S ($\simeq 1374\,W.m^{-2}$), α_S, Δ_S, i_S, p and p_o($= 101325$ Pa) are the solar constant, the alleviation coefficient of solar radiant flux through the atmosphere, the coefficient of variation due to the distance Earth-Sun, incidence under which the cells see the Sun, static pressure at altitude considered and that on the level of the Earth, respectively.

The modelling of the atmosphere appears indirectly in the air density.

3 Aircraft

3.1 Drag model

Total drag coefficient C_D is the sum of zero-lift drag coefficient C_{D_0} and induced drag :

$$C_D = C_{D_0} + \frac{1}{\pi \lambda} {C_L}^2$$

where $\lambda = b/l$, C_L, b and l are the wing aspect ratio, the lift coefficient, the wingspan and the aerofoil chord, respectively. The drag coefficient without lift is assumed to be equal to the sum of drag due to the aerofoil form and those of the body. Models are elaborate in [8].

3.2 Electric motor mass

The mass of the engines is defined by the maximum useful power $P_{u_{max}} = F_{max} V_c$ where V_c is the cruising velocity and F_{max} is the maximum thrust. Maximum thrust is defined by the ceiling of propulsion such as $F_{max} = mg/f$ where f is the lift to drag ratio. For a specific mass M_{mot} (mass of the engines/maximum power), the mass of the engines can be written in the following form:

$$m_{mot} = M_{mot} \frac{mg}{f} \frac{V_c}{\eta_H} \tag{1}$$

where η_H is the propeller efficiency. The specific power of the engines is supposed to be constant for all studied UAVs.

3.3 Photovoltaic cell mass

The solar radiance power $P_S = \overline{P_S} S_{cel}$ is transformed in electric power P_{elec} by the solar cells with an efficiency η_{cel}. Then, electric power is consumed by payload power $P_{payload}$ and electric motor power P_{mot} with an efficiency η_{mot}. We have:

$$P_{elec} = \frac{P_{mot}}{\eta_{mot}} + P_{payload} = \eta_{cel} P_S \tag{2}$$

Let us note that the night operation is not taken into account in modelling. Thus, with Eq.(1) and let us note the cell surface density $\varpi_{cel} = m_{cel}/S_{cel}$, we can obtain the mass of the cells:

$$m_{cel} = \frac{\varpi_{cel}}{\eta_{cel} \overline{P_S}} \left(\frac{1}{\eta_H \eta_{mot}} \frac{mg}{f} V_c + P_{payload} \right) \tag{3}$$

3.4 Wing mass

3.4.1 Wing design

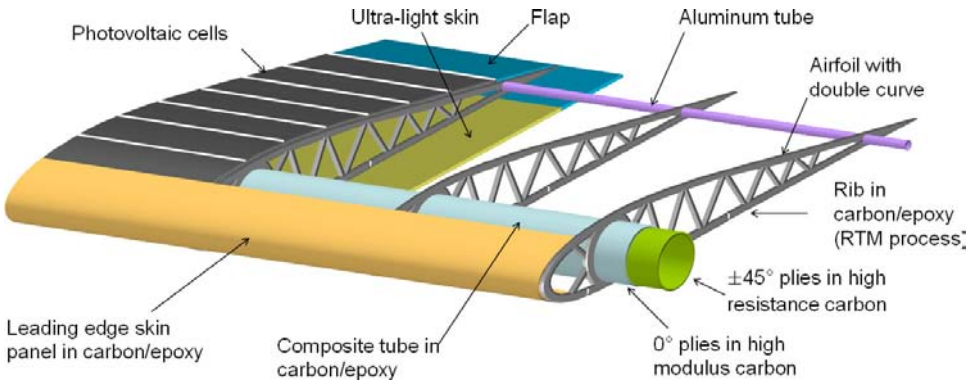

Figure 2: Sketch of the wing configuration called "tubular structure"

Models used in the optimisation problem need to have a physical sense for a wide range of solar-powered HALE UAVs. In particular, the wing mass model needs to have a technological sense for a wide range of wing surfaces. In other word, this model must be generic. The wing architecture proposed is a "tubular structure" (Fig. 2). The wing with rectangular form is constituted of :

- a tubular beam with non-constant cross sections and constant composite laminate stacking sequence. At the wing-root, inner and outer radius are r_{i_0} and r_{o_0}, respectively. The wing-root outer radius is defined by the expression $r_{o_0} = \epsilon_r \epsilon_e l/2$ where $\epsilon_r < 1$, e and $\epsilon_e = e/l$ are the relative diameter of

the beam, the aerofoil thickness and the relative aerofoil thickness, respectively. The parameter κ characterised the linear variation of radius along the wing i.e. $r_o(y) = r_{o_0}\left(1 - \kappa\frac{2}{b}y\right)$ with $\kappa \in [0, 1]$, $y \in [0, b/2]$;

- ultra-light ribs in composite materials (for example, made with RTM process), their total mass is $m_{rib} \approx n_{rib}\varpi_{rib}le/2$ where $n_{rib} = \mathrm{E}(2b)$ is the number of ribs (E is the entier function) and ϖ_{rib} is the mass of the rib per unit area ;

- ultra-light skins, their total mass is $m_{skin} \approx \varpi_{skin}b(2l + e)$ where ϖ_{skin} is the mass of the skin per unit area ;

- secondary parts like components of hinged surfaces, local reinforcements, small tubular beam to rigidify the trailing edge of the wing, ... their total mass is $m_{remw} = \xi_{remw}m_w$ where m_w and $\xi_{remw} < 1$ are the mass of the wings and the percentage of mass of the secondary parts in the wing, respectively.

Main beam is assumed to be the only part that bear aerodynamic and inertial forces. If beam was constituted of homogeneous material like aluminium, the optimisation would be only the computation of geometric parameters [9]. Nevertheless, the specific modulus (Young's modulus/density) of homogeneous materials is not enough large to obtain a lightweight structure. In modern aircraft structures, carbon/epoxy laminates are preferred because specific modulus can be five times larger. This material is chosen for the beam. In this case, the optimisation is more complex and choices should be made like parameters of the stacking sequence, carbon fibres, parameters of the beam, ... These choices are not necessary if an optimisation algorithm of the stacking sequence is used like a genetic algorithm well adapted for the stacking sequence search [10].

Here, we choose a generic stacking sequence well adapted to bending and torsion problems: $[0^\circ_{n_0}, \pm 45^\circ_{n_{\pm 45}}]$ where n_0 and $n_{\pm 45}$ are the unknown number of 0° and ±45° plies, respectively (Fig. 3). This laminate has the advantage to approximately uncoupled the flexural resistance problem and torsional resistance problem. It is well known that 0° plies are the stiffness and strength optimum for a composite beam in bending as well as ±45° plies are the stiffness and strength optimum for a composite beam in torsion. If 0° plies and ±45° plies are constituted of various fibres with the same epoxy resin, the composite material is called *hybrid carbon/epoxy material*. For example, high modulus carbon fibres used for 0° plies can increase widely the flexural wing stiffness. High resistance carbon fibres used for 0° plies can increase the wing strength in tension and compression.

The aim of the wing optimisation is to minimise the total number of plies (n_0 and $n_{\pm 45}$) and to maximise the parameter κ to minimise the mass of the main beams. If $\kappa = 0$, the mass is $m_{beam0} = \rho_0\pi b(r_{o_0}^2 - r_{f_0}^2) + \rho_{\pm 45}\pi b(r_{f_0}^2 - r_{i_0}^2)$ where ρ_i is the mass density of the ply i and r_{f_0} is the boundary radius of the beam between 0° and ±45° plies. If $\kappa \in]0, 1]$ and $\frac{t}{r_{o_0}} = 1 - \frac{r_{i_0}}{r_{o_0}} \ll 1$, the mass of the beam is $m_{beam} \approx \frac{2-\kappa}{2}m_{beam0}$ where t is the thickness of the beam.

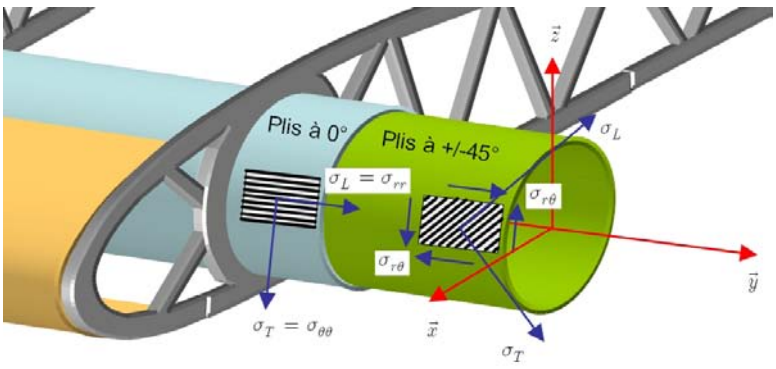

Figure 3: Laminates orientations

3.4.2 Forces and moments

To simplify dramatically the modelling and minimise dynamical coupling effects between bending and torsion, the centre of gravity of a wing section is assumed to be located at the centre of the beam cross section which is located at the aerodynamic centre of the aerofoil (approximately quarter-chord point).

The forces acting on a wing section are composed of aerodynamic forces and inertial forces. The first can be decomposed in two parts, one part provided by the aerofoil and the second one provided by the position of ailerons. The general case of sizing loads, i.e. JAR22 adapted to HALE UAVs, is presented in [11]. A simplified formulation is proposed here to obtain an analytical wing mass model with several assumptions: same aerofoil for all sections ; rectangular wing ; lifting and moment coefficient of the wing equal to that of the aerofoil ; lift provided only by the wing.

The first loading case is design at extreme load factor (turning flight stall), where $V = V_{\max}$, $C_{\mathrm{L}} = C_{\mathrm{L}_{\max}}$. The stall load factor $n_{\max}$ is replaced by the extreme load factor n_{ext} to take into account of a safety factor and gust effects. Then, the extremal force and moment per unit of wingspan applied at the centre of the beam cross section can be written:

$$\mathcal{F}_{\text{ext}} = (m - m_w - m_{mot})\frac{n_{\text{ext}} g}{b} \; ; \; \mathcal{M}_{\text{ext}} = m\frac{n_{ext} g l}{b}\frac{C_{\mathrm{M}_o}}{C_{\mathrm{L}_{\max}}} \tag{4}$$

where m and g are the total mass of the UAV and the acceleration due to gravity, respectively. The second loading case is design aileron down limit speed. In this case, we consider the asymetric load factor $n_{asym} = \frac{2}{3} n_{ext}$. The size of the aileron is computed before to obtain a turn of 180°, with a pitch angle of 45°, at a velocity of $1.4V_{s1}$ in $b/3$ seconds where V_{s1} is the velocity at stall limit for $n = 1$. The maximal moment is obtained at extremal position of the ailerons. Then, the asymetric force and moment per unit of wingspan applied at the centre of the beam cross section can be written:

$$\mathcal{F}_{asym} = (m - m_w - m_{mot})\frac{n_{asym} g}{b} \; ; \; \mathcal{M}_{asym} = m\frac{n_{asym} g l}{b}\frac{C_{\mathrm{M}_o} + C_{\mathrm{M}_{\delta_m}}\delta_m}{C_{\mathrm{L}_{\max}}} \tag{5}$$

where C_{M_o}, $C_{\mathrm{M}_{\delta_m}}$ and δ_m are the pitching moment coefficient at the aerodynamic centre, the pitching govern efficiency coefficient and the pitching govern amplitude, respectively.

3.4.3 Stress analysis

We work with the beam theory and material is assumed to be linear elastic. The small thickness of the tubular beam comparatively to the radius allows us to assume a plane stress field in the skin of the tube. Therefore, we can work with a simplified laminate theory which assume that coupling effect between 0° and ±45° plies is negligible. It is clear that computation results need to be verified with the classical laminate theory [12] after optimisation.

With these important assumptions and Eq. (4), we can write the maximum/minimum stress in the 0° plies at the root of the wing due to first loading case:

$$\sigma_{\max.0} = \frac{E_{yy_0} r_{o_0} b}{8(EI)_{yy_{\text{hom}}}} n_{\text{ext}}(m - m_v - m_{mot})g = -\sigma_{\min.0} \tag{6}$$

with

$$(EI)_{yy_{\text{hom}}} = \frac{\pi}{4}\left[E_{yy_0}\left(r_{o_0}^4 - r_{f_0}^4\right) + E_{yy_{\pm 45}}\left(r_{f_0}^4 - r_{i_0}^4\right)\right] \approx \pi r_{o_0}^3 t_{\text{ply}}\left[n_0 E_{yy_0} + 2n_{\pm 45} E_{yy_{\pm 45}}\right] \tag{7}$$

where E_{yy_i} is the tensile modulus in the y direction for the ply i (Fig. 3). With Eq. (5), we can write the maximum stress in the ±45° plies at the root of the wing due to second loading case:

$$\sigma_{\max.\pm 45} = \frac{E_{yy_{\pm 45}} r_{f_0} b}{8(EI)_{yy_{hom}}} n_{asym}(m - m_w - m_{mot})g = -\sigma_{\min.\pm 45} \tag{8}$$

$$\tau_{\max.\pm 45} = \frac{E_{xy_{\pm 45}} r_{f_0} l}{2(EJ)_{xy_{\text{hom}}}} n_{asym} mg \frac{C_{\mathrm{M}_o} + \frac{b_a}{b} C_{\mathrm{M}_{\delta_m}}\delta_m}{C_{\mathrm{L}_{\max}}} \tag{9}$$

with

$$(EJ)_{xy_{\text{hom}}} = \frac{\pi}{2}\left[E_{xy_0}\left(r_{o_0}^4 - r_{f_0}^4\right) + E_{xy_{\pm 45}}\left(r_{f_0}^4 - r_{i_0}^4\right)\right] \approx 2\pi r_{o_0}^3 t_{\text{ply}}\left[n_0 E_{xy_0} + 2n_{\pm 45} E_{xy_{\pm 45}}\right] \tag{10}$$

where E_{xy_i} is the shear modulus in the xy direction for the ply i and b_a is the total length of the ailerons.

3.4.4 Strength criterion

It is well known that carbon/epoxy materials can encountered various damage process (matrix damage due to mechanical stress, thermal stress and hydrometry) and rupture process (fibre fracture, delamination, interface decohesion, local buckling ...) complex to modelled [13]. For the UAV optimisation, the strength computation must be as simple as possible. Strain or a stress criterion are well adapted. Here, we work with the Tsai-Wu criterion [12] which can be written in the ply coordinate system :

$$\frac{\sigma_L^2}{XX'} - \frac{\sigma_L \sigma_T}{\sqrt{XX'YY'}} + \frac{\sigma_T^2}{YY'} + \frac{\sigma_{LT}^2}{C^2} + \left(\frac{1}{X} - \frac{1}{X'}\right)\sigma_L + \left(\frac{1}{Y} - \frac{1}{Y'}\right)\sigma_T = 1 \tag{11}$$

where L, T and LT signify longitudinal, transverse and in-plane shear ; X , X', Y, $Y'$and C are maximal strength in longitudinal tension, in longitudinal compression, in transverse tension, in transverse compression and in in-plane shear, respectively.

For the first loading case and for the 0° plies, local stress are: $\sigma_L = \sigma_{yy}$, $\sigma_T = \sigma_{\theta\theta} = 0$ and $\sigma_{LT} = \sigma_{y\theta} = 0$. Therefore,Tsai-Wu criterion is written in the following form:

$$\frac{1}{XX'}\sigma_{yy}^2 + \left(\frac{1}{X} - \frac{1}{X'}\right)\sigma_{yy} = 1 \quad \Rightarrow \quad (\sigma_{yy} - X)(\sigma_{yy} + X') = 0 \tag{12}$$

Classically in carbon/epoxy materials, the longitudinal strength in tension is higher than in compression $X \geqslant X'$ then criterion can simply rewrite in a constraint form

$$\sigma_{\max.0} \leqslant X' \tag{13}$$

In the case of this simplified approach, it can be assumed that fibre fracture in the 0° plies happen before the fracture in the ±45° plies, because maximal strain of 0° plies is lower than ±45° plies. This hypothesis is conservative.

For the second loading case and for the ±45° plies, it is necessary to write the criterion in the ply coordinate system that is computing shear stress in a coordinate system at 45° (or −45°) relatively to $\vec{y}$. This coordinate system rotation gives the following local stress: $\sigma_L = \frac{\sigma_{yy}}{2} + \sigma_{y\theta}$, $\sigma_T = \frac{\sigma_{yy}}{2} - \sigma_{y\theta}$ and $\sigma_{LT} = -\frac{\sigma_{yy}}{2}$. Therefore, Tsai-Wu criterion is written in the following form:

$$\tfrac{1}{4}\left(\tfrac{1}{XX'} - \tfrac{1}{\sqrt{XX'YY'}} + \tfrac{1}{YY'} + \tfrac{1}{C^2}\right)\sigma_{\max\pm.45}^2 + \underbrace{\left(\tfrac{1}{XX'} + \tfrac{1}{\sqrt{XX'YY'}} + \tfrac{1}{YY'}\right)}_{A}\tau_{\max\pm.45}^2 \tag{14}$$

$$+\tfrac{1}{2}\left(\tfrac{1}{X} - \tfrac{1}{X'} + \tfrac{1}{Y} - \tfrac{1}{Y'}\right)\sigma_{\max\pm.45} + \underbrace{\left(\tfrac{1}{X} - \tfrac{1}{X'} - \tfrac{1}{Y} + \tfrac{1}{Y'}\right)}_{B}\tau_{\max\pm.45} = 1 \tag{15}$$

In the case of this simplified approach, longitudinal stress in ±45° plies are neglected. Moreover, in carbon/epoxy materials, strength in transverse compression is higher than in tension *i.e.*, $Y' \geqslant Y$. With previous $X \geqslant X'$ assumption, we have $A \geqslant 0$ and $B \leqslant 0$. Then, Tsai-Wu criterion can be written in the following form:

$$\tau_{\max.\pm 45} \leqslant \frac{B + \sqrt{B^2 + 4A}}{2A} \tag{16}$$

Finally, after some calculations and assuming $\frac{t}{r_{o_0}} \ll 1$ and $\kappa = 0$, the validation of Eqs. (13) and (16) can be rewritten in the following form that gives directly number of 0° plies and ±45° plies in an analytical form:

$$n_{\pm 45} = \mathsf{UpRd}\left(\frac{\frac{E_{xy_0}(m-m_{mot}-m_{skin}-m_{rib})}{2\pi r_{o_0} t_{\text{ply}}\left(\frac{4r_{o_0}X'}{bn_{\text{ext}}g}+b(1+\xi_{remw})\rho_0\right)} - \frac{E_{xy_{\pm 45}} l n_{asym} mg}{4\pi r_{o_0}^2 t_{\text{ply}} D}\frac{\text{CM}_o+\frac{b_a}{b}\text{CM}_{\delta_m}\delta_m}{\text{CL}_{2/3}}}{2\frac{\frac{4r_{o_0}X'}{bn_{\text{ext}}g}\frac{E_{yy_{\pm 45}}}{E_{yy_0}}+b(1+\xi_{remw})\rho_{\pm 45}}{\frac{4r_{o_0}X'}{bn_{\text{ext}}g}+b(1+\xi_{remw})\rho_0}E_{xy_0} - 2E_{xy_{\pm 45}}}\right) \tag{17}$$

$$n_0 = \mathsf{UpRd}\left(\frac{\frac{E_{xy_{\pm 45}}(m-m_{mot}-m_{skin}-m_{rib})}{2\pi r_{o_0} t_{\text{ply}}\left(\frac{4r_{o_0}X'}{bn_{\text{ext}}g}\frac{E_{yy_{\pm 45}}}{E_{yy_0}}+b(1+\xi_{remw})\rho_{\pm 45}\right)} - \frac{E_{xy_{\pm 45}} l n_{asym} mg}{4\pi r_{o_0}^2 t_{\text{ply}} D}\frac{\text{CM}_o+\frac{b_a}{b}\text{CM}_{\delta_m}\delta_m}{\text{CL}_{2/3}}}{\frac{\frac{4r_{o_0}X'}{bn_{\text{ext}}g}+b(1+\xi_{remw})\rho_0}{\frac{4r_{o_0}X'}{bn_{\text{ext}}g}\frac{E_{yy_{\pm 45}}}{E_{yy_0}}+b(1+\xi_{remw})\rho_{\pm 45}}E_{xy_{\pm 45}} - E_{xy_0}}\right) \tag{18}$$

where UpRd(.) is the upper round-off function.

Buckling risk in torsion is not taken into account in this paper. To avoid local buckling risk, a thickness constraint is set $t = r_e - r_i \leqslant t_{\min}$ where $t_{\min}$ is the minimal thickness of the beam.

3.4.5 Wing flexibility

A wing which satisfies the strength criterion can be too largely flexible, which strongly deteriorate the aircraft performances. This phenomenon is as much more significant than the wing has a large aspect ratio. This deformation implies a lift reduction and causes a parasitic drag. It is necessary to define a displacement criterion *i.e.*, a maximal displacement of the wing tip : $u_{z.\max} \leqslant \Lambda_{\max}\frac{b}{2}$ where $\Lambda_{\max}$ is the relative maximal displacement. With Euler-Bernoulli assumption with a constant stacking sequence but linearly decreasing cross section, the displacement is written after some computations:

$$u_{z.\max} = \frac{n_{\text{ext}} g b^3}{128(EI)_{yy_{\text{hom}}}}\left(4\frac{m-m_{mot}-m_{skin}-m_{rib}}{m_{beam0}} - 2 + \kappa\right)\frac{6(1-\kappa)\ln(1-\kappa)+6\kappa-3\kappa^2-\kappa^3}{2\kappa^4} \tag{19}$$

Finally, the following criterion gives the parameter κ:

$$\text{find}\,\kappa \in [0,1] / \; u_{z.\max} - \Lambda_{\max}\frac{b}{2} = 0$$

3.5 Remaining structural mass

The mass of the fuselage is expressed with the Roskam model: $m_{fus} = 0.232\ m^{0.95}$ [14]. Lastly, mass of the tail and the landing gear are supposed to be proportional to the total mass *i.e.*, $m_{tail} = \xi_{tail} m$ and $m_{gear} = \xi_{gear} m$. We note $m_{rem} = m_{fus} + m_{gear} + m_{tail}$.

4 Merit function and conceptual constraints

The total mass of the UAV is:

$$m = m_w + m_{mot} + m_{cel} + m_{rem} + m_{payload} \quad \text{with} \quad m_w = m_{beam} + m_{rib} + m_{skin} + m_{remw} \tag{20}$$

where $m_{payload}$ is the mass of the payload. This mass is the variable to maximise. Then, a merit function $\mathcal{MF}$ to minimise can be obtained:

$$\frac{m_{payload}}{m} = 1 - \frac{m_w + m_{mot} + m_{cel} + m_{rem}}{m} = 1 - \mathcal{MF} \tag{21}$$

It is clear that $m_{payload} > 0$ *i.e.*,

$$\mathcal{MF} \leq 1 \tag{22}$$

The second constraint is the solar cells total surface S_{cel} which must be inferior to the wing surface. In other word, the cell occupancy rate $\mathcal{T} = S_{cel}/S$ must be inferior to the maximal occupancy rate $\mathcal{T}_{\max}$:

$$\mathcal{T} \leq \mathcal{T}_{\max} \tag{23}$$

Table 1: UAV conceptual properties

m_{mot}	η_{mot}	η_H	η_{cel}	ϖ_{cel}	ϖ_{skin}	ϖ_{ri}	ϵ_e	ϵ_r
$N.kW^{-1}$	-	-	-	$kg.m^2$	$kg.m^2$	$kg.m^2$	-	-
32	0.9	0.9	0.13	0.45	0.1	4.8	0.12	0.9

$\Lambda_{\max}$	$\xi_{rem\,w}$	ξ_{tail}	ξ_{gear}	$t_{\min}$	$C_{L\max}$	C_{M_o}	$C_{M_{\delta_m}}$	δ_m	n_{ext}
-	-	-	-	mm	-	-	-	°	-
0.16	0.1	0	0.032	1.5	1.4	0.05	0.5	10	3.1

Table 2: T800/M18 properties for a 0.6 volume fraction

ρ	$E_{11} = E_{yy\,0}$	E_{22}	$E_{66} \approx E_{xy\,0}$	E_{12}	$E_{yy\,\pm45}$	$E_{xy\,\pm45}$	X	X'	Y	Y'	S	t_{ply}
$kg\,m^{-3}$	GPa	GPa	GPa		GPa	GPa	MPa	MPa	MPa	MPa	MPa	mm
1 530	162	10	5.0	0.3	13.2	9.1	2 940	1 570	60	290	100	0.125

5 UAV optimisation

The optimisation process corresponds to a Torenbeek method [15]. The maximum take-off weight and the endurance are fixed therefore the mass of payload has to be maximised. Here, the endurance is not under consideration because the UAV is assumed at a flight point and there is no problem of fuel consumption.

The number of parameters is large and it is impossible to study the effect of all. A selection is made to choose relevant conceptual parameters. For this study, the wing aspect ratio λ and the maximum take-off weight m are fixed to 12.5 and 220 kg, respectively, which corresponds to «Pathfinder» prototype [6]. The parameters scanned with the algorithm are the cruise speed V_c and the lift coefficient C_L which is directly proportional to the wing surface.

The cruise altitude h is chosen equal to 60 000 ft. The position of the UAV is the France at the latitude of 45° and the time is the 22th of June at 12 h *i.e.*, the summer solstice. The maximal occupancy rate of photovoltaic cells $\mathcal{T}_{\max}$ is 75 %. This value allows to distribute cells on the main part of the surface without the edges with high curvature. Maximal occupancy rate could be increased up to 90%. Other parameters of the UAV are given in the Tab. 1. Then, the carbon/epoxy of the beam is a T800/M18 which properties are defined in Tab. 2.

Finally, the diagram of the algorithm is given in Fig. 4.

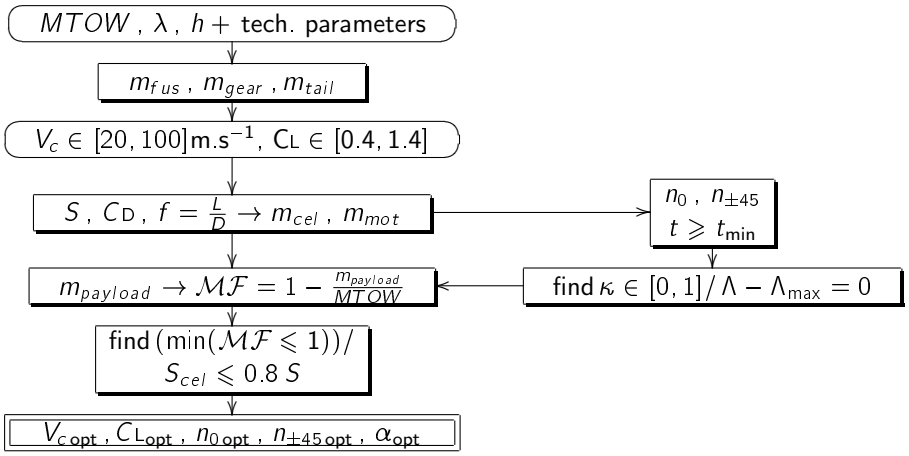

Figure 4: Algorithm diagram to compute the optimised UAV

Table 3: Optimal UAV definition

S	b	l	c_a	m_w	m_{mot}	m_{cel}	m_{rem}	$m_{payload}$	m_{beam}	m_{skin}	m_{rib}	m_{remw}	n_0	$n_{\pm 45}$
m^2	m	m	$kg.m^2$	kg	kg	kg	kg	kg	kg	kg	kg	kg	-	-
45.9	23.9	1.9	4.8	105.8	12.8	15.4	57.1	28.9	35.9	9.7	50.6	9.6	2	5

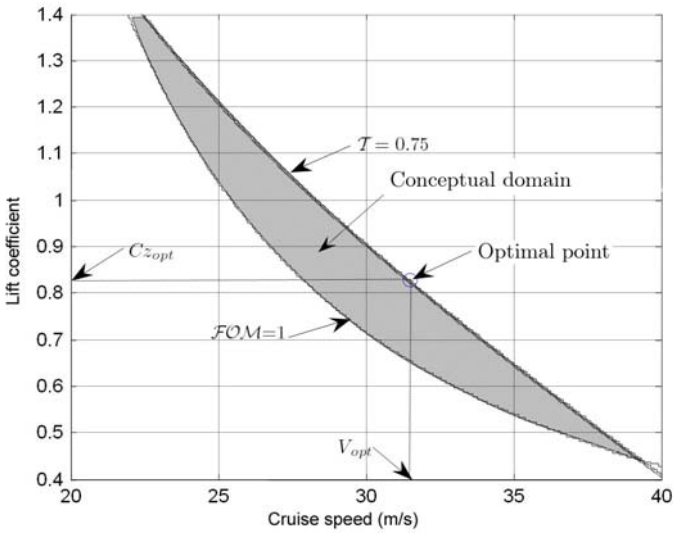

Figure 5: Existence domain of the solar-powered HALE UAV (domain in grey) in a cruise speed versus lift coefficient diagram.

6 Results

The contour of $\mathcal{MF}$ and $\mathcal{T}_{\max}$ functions are plotted in the (V_c ; C_L) axes (Fig. 5). The constraint on the occupancy rate of photovoltaic cells decrease dramatically the feasibility domain. The merit function get a minimum called optimal point, approximately 0.9. The optimal point ($V_{opt} \approx 31 m.s^{-1}$; $C_{L_{opt}} \approx 0.85$) is on the $\mathcal{T} = \mathcal{T}_{\max}$ curve, which is not surprising. At this point, the mass of payload represents approximately 29 kg for a maximal take-off mass of 220 kg. The optimal velocity is over the maximum gusts. Other characteristics of the HALE are given in the Tab. 3.

7 conclusion

Optimisation carried out here consists in maximising the payload for a fixed total mass. It requires mass model for each constitutive part of the aircraft. In particular, the mass of the wing is minimised by the use of composite materials and by tolerate a large flexibility. An new analytical mass model is proposed here very useful for this particular application.

Optimisation shows the existence of the Solar-powered HALE UAV in a cruise speed versus lift coefficient diagram. This one revealed an optimal solution having a payload of about 13 % of the total mass of 220 kg for a 24 m wing span. Noting that computation is made with several pessimistic parameter values (low occupancy rate of photovoltaic cells, low efficiency of solar cells, high load factor) and several optimistic parameter values (day, hour).

This work needs to be continued to optimise the effect of wing aspect ratio. Then, the sizing during night operation in the aim to flight weeks to months will necessitate to add an energy storage system. Finally, an endurance computation will be realised.

References

[1] S. R. Herwitz, L. F. Johnson, J. C. Arvesen, R. G. Higgins, J. G. Leung, S. E. Dunagan, Precision agriculture as a commercial application for solar-powered unmanned aerial vehicles, in: 1st Unmanned Aerospace Vehicles, Systems, Technologies, and Operations Conference and Workshop, Portsmouth, VA, 2002.

[2] M. Harmats, D. Weihs, Hybrid-propulsion high-altitude long-endurance remotely piloted vehicle, Journal of Aircraft 36 (2) (1999) 321–331.

[3] B. Keidel, Design of a solar-powered hale aircraft for year-round operation at intermediate latitudes, in: Proceeding of the RTO symposium on "UV for aerial, ground and naval military operations", Ankara, Turkey, 2000.

[4] G. Romeo, G. Frulla, E. Cestino, G. Corsino, Heliplat: Design, aerodynamic and structural analysis of very-long endurance solar powered stratospheric uav, Journal of Aircraft 41 (6) (2004) 1505–1520.

[5] S. V. Serokhvostov, T. E. Churkina, Optimal control for the sunpowered airplane in a multiday mission, in: 2nd European Conference for Aerospace Sciences (EUCASS), Brussells, Belgium, 2007.

[6] K. Flittie, B. Curtin, Pathfinder solar-powered aircraft flight performance, in: Proceeding of the AIAA Atmospheric Flight Mechanics Conference & Exhibit, Boston, 1998.

[7] T. Noll, J. Brown, M. Perez-Davis, S. Ishmael, G. Tiffany, M. Gaier, N. Headquarters, Investigation of the helios prototype aircraft mishap: Volume i mishap report, nasa, Tech. rep. (2004).

[8] L. Bovet, Optimisation conceptuelle de la croisière - application aux avions de transport civils, Ph.D. thesis, University of Marseille, France (2004).

[9] L. Bovet, O. Montagnier, Optimisation conceptuelle d'un drone à énergie solaire, Tech. rep., CReA (2006).

[10] O. Montagnier, C. Hochard, Optimization of supercritical carbon/epoxy drive shafts using a genetic algoritm, in: Proceedings of the 13th European Conference on Composite Materials, Stockholm, Sweden, 2008.

[11] J. Raska, Pertinence des modèles de conception d'un avant-projet d'avion – application aux gnoptères hale, Ph.D. thesis, ENSAE (2000).

[12] S. W. Tsai, E. M. Wu, A general theory of strength of anisotropic materials, Journal of Composite Materials 5 (1971) 58–69.

[13] C. Hochard, J. Payan, O. Montagnier, Design and computation of laminated composite structures, Composites Science and Technology 65 (2005) 467–474.

[14] J. Roskam, Airplane Flight Dynamics and Automatic Flight Controls, Darcorporation, 2001.

[15] E. Torenbeek, Synthesis of subsonic airplane design, Delft University Press, 1988.